Confinement-Induced Deviation of Chain Mobility and Glass Transition Temperature for Polystyrene/Au Nanoparticles

ARTICLE *in* MACROMOLECULES · MARCH 2013

Impact Factor: 5.8 · DOI: 10.1021/ma302643y

6 AUTHORS, INCLUDING:

Xiaoliang Wang
Nanjing University
45 PUBLICATIONS **283** CITATIONS
SEE PROFILE

Wei Chen
Central South University
539 PUBLICATIONS **15,520** CITATIONS
SEE PROFILE

Pingchuan Sun
Nankai University
119 PUBLICATIONS **1,543** CITATIONS
SEE PROFILE

Macromolecules

Article

pubs.acs.org/Macromolecules

Confinement-Induced Deviation of Chain Mobility and Glass Transition Temperature for Polystyrene/Au Nanoparticles

Lili Zhu,[†] Xiaoliang Wang,[†] Qiang Gu,[†] Wei Chen,[†] Pingchuan Sun,[‡] and Gi Xue*,[†]

[†]Department of Polymer Science and Engineering, The School of Chemistry and Chemical Engineering, The State Key Laboratory of Coordination Chemistry, Nanjing University, Nanjing 210093, P. R. China

[‡]Key Laboratory of Functional Polymer Materials, Ministry of Education, Nankai University, Tianjin 300071, P. R. China

Supporting Information

ABSTRACT: The mobility and glass transition temperature (T_g) for polymers under nanoscale confinement differ substantially from the bulk. Whereas many studies have focused on the one-dimensional confinement, it has great significance to extend studies to higher geometries. Here, we systematically investigate the mobility by dipolar-filter sequence in solid-state NMR and T_g by DSC for thiolated polystyrene (PS-SH) on gold nanoparticles. The increase in T_g and signal suppression in NMR spectra clearly indicate that the surface confinement dominates molecular mobility as well as T_g. The molecular weight of PS-SH and nanoparticles size show significant influence on the immobilization and T_g. Our results can be fitted with a core−two shell model; the inner shell is under strong constraints while the outer shell with less confinement. This work is essential to better understand the confinement effect and also provides a step toward the ultimate desire to tailor the properties of nanomaterials.

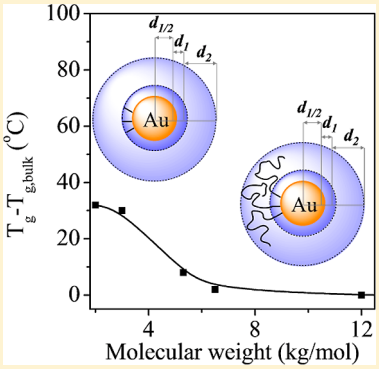

INTRODUCTION

The mobility and thermal dynamic properties of polymers when confined at nanometer length scales differ greatly from properties in the bulk.[1−11] By using fluorophores to label a single layer within a multilayer polystyrene (PS) film, Ellison and Torkelson[1] performed the first direct measurement of glass transition temperature (T_g) gradients in substrate-supported PS films. Paeng and Ediger et al.[6] measured the molecular mobility in free-standing polystyrene films dispersed with fluorescent probe by an optical photobleaching technique. The effects of such nanoscale confinement on molecular mobility/T_g have gathered substantial academic and industrial interest due to their potential applications in advanced nanotechnology, such as nanocomposites, biomolecules, and optical and electrical materials.[12−19] Shin and Russell et al.[20] pointed out that nonclassical behavior brought about by a physical confinement that imposes special constraints on molecular motion is opening avenues to surface science. However, there still is a remarkable paucity about fundamental descriptions of mobility under nanoconfinement. Descriptions are complicated not only by the effects of the confinement on molecular interactions and conformation but also by molecular interactions with the confining surfaces.[15,21−23] Meanwhile, the deviation of T_g from the bulk, i.e., T_g-confinement effect, has been studied in the past two decades by a great number of reports with no general consensus revealed in the literature.[11,24−26] With the interest in determining the generality of the T_g-confinement effect, people considered the correspondence between the behaviors of polymer thin film and polymers confined to higher geometrical dimensionalities, such as polymer on nanoparticles and in nanopores.[12−14,27−34] Recently, Zhang and Priestley et al.[27] investigated the size dependence of T_g for three-dimensional confined system PS nanoparticles under soft and hard confinement, finding a striking similarity of size-dependent effects on the T_g for polymer nanoparticles and free-standing films. However, as compared to thin film, polymer-capped nanoparticles and nanocomposites are typically harder to design and characterize, and much less fundamental understanding exists regarding the mobility of chains capped on nanoparticles.[35−39]

The knowledge about the mobility of ligands on nanoparticles is limited, due in part to the obscure of spectroscopic signals for the moieties nearest to the surface of solid. Nuclear magnetic resonance (NMR) spectroscopy is particularly informative, as for all molecular compounds, for the part of the ligands remote from the core.[38−41] Lennox and Reven et al. successfully investigated structure and property for the assembled monolayer by a diverse range of materials characterization techniques with an emphasis on NMR spectroscopy.[35−40] It has been pointed out that the solution ^{1}H and ^{13}C NMR resonance of the moiety nearest to Au are characteristically broadened, downfield-shifted, or even completely disappeared.[35−38] The reasons for the peak broadening or resonance disappearance, which impedes an exact quantitative analysis and restricts the measurement for organic−inorganic interface, are still subject to discussion.[42−44] ^{13}C solid-state NMR (SSNMR) is a powerful method for structural analysis of noncrystalline solids. However, ^{13}C SSNMR requires larger

Received: December 26, 2012
Revised: February 5, 2013
Published: March 4, 2013

amounts of samples (0.1−1 mmol) compared with ^{1}H NMR because of low abundance of ^{13}C. ^{1}H SSNMR is an attractive alternative to ^{13}C SSNMR, particularly for unlabeled systems and samples in limited quantities because of its high sensitivity.[43,44] In ^{1}H high-resolution SSNMR, multiple-pulse ^{1}H−^{1}H dipolar decoupling has been required, together with magic angle spinning (MAS) to suppress line broadening due to strong ^{1}H−^{1}H couplings.[42,43]

Recently, our group demonstrated a new approach to obtain high-resolution ^{1}H SSNMR of polymer systems using very fast MAS (VFMAS; spinning speed >20 kHz).[21−23] We define VFMAS as above because MAS at 20 kHz or more induces crucial changes in the spin dynamics for organic solids by eliminating the majority of dipolar couplings. It is observed that NMR T_2 relaxation time for ligands on NPs is dramatically altered due to the restrictions on mobility that the ligands experience in the vincity of the surfaces. However, because of the signal oscillations under MAS, T_2 cannot be utilized to characterize the mobility of confined polymers in our system (see Figures S1 and S2 in the Supporting Information). A 12-pulse dipolar filter NMR experiment developed by Schmidt-Rohr[45−47] was used to select the ^{1}H magnetization with a weak dipole−dipole interaction. This method has also been applied to distinguish a "mobile" component which has weaker dipolar interaction compared to the rigid ones. In particular, dipolar filter experiment reflects dynamic heterogeneity over shorter scales than those measured by traditional relaxation NMR experiments.[43,45−49]

In the present work, we focused on the confinement-induced chain mobility and T_g deviation for thiolated polystyrene adsorbed on gold nanoparticles (PS-S-Au NPs) by the use of ^{1}H SSNMR spectroscopy and differential scanning calorimetry (DSC). Polymer monolayer capped NPs seem particularly valuable here since they not only represent a unique high geometrical nanoconfined polymer system but also can serve as fillers in another nanoconfined system, polymer nanocomposites (PNCs). Here, we systemically explored the size effect (NPs size and molecular weight) on chain mobility and ΔT_g ($T_g - T_{g,bulk}$) for polystyrene thiolate (PS-S-) on Au NPs. When PS-S- with low molecular weight adsorbed on Au NPs, the mobility was reduced and T_g for PS was found to increase significantly, due to the strong confinement between polymer chains and Au NPs. The deviation of chain mobility and T_g increased with increased particle size. Meanwhile, its related PNCs exhibited substantially increased T_g than bulk PS-SH. However, for high molecular weight PS-SH, undetectable changes in PS-S- mobility and T_g for PS−S-Au NPs/PNCs were observed. This work enabled us to enhance the understanding of confinement effect and better regulate the properties of nanomaterials.

EXPERIMENTAL SECTION

Materials. Sodium borohydride ($NaBH_4$, 99%) and hydrogen tetrachloroaurate ($HAuCl_4{\cdot}3H_2O$) were purchased from Sigma-Aldrich Co. Thiol-terminated polystyrene PS-SH (M_n = 2000 g/mol, M_w/M_n = 1.15; M_n = 3000 g/mol, M_w/M_n = 1.07; M_n = 5300 g/mol, M_w/M_n = 1.10; M_n = 6500 g/mol, M_w/M_n = 1.18; M_n = 12 000 g/mol, M_w/M_n = 1.09) were purchased from Polymer Source. All of the solvents were commercial available and distilled before use. All glasswares were cleaned with aqua regia (HCl:HNO_3 = 3:1 vol %), rinsed with copious amounts of ultrapure water, and then dried in an oven prior to use.

One-Phase Synthesis of Thiolated Polystyrene-Capped Au NPs. Thiolated polystyrene PS-SH was mixed with $HAuCl_4{\cdot}3H_2O$ in 10 mL of freshly distilled tetrahydrofuran (THF). The color of the solution was pale yellow. A solution of 0.01 mol/L $NaBH_4$ dissolved in 10 mL of mixed solvents of THF−water was added to the solution under vigorous stirring. The color of the solution turned dark red-brown immediately. Then the solution was stirred at room temperature for 3 h. Reaction conditions (thiol/Au ratio, rate of reductant addition) have been controlled to prepare PS-S-Au NPs with different size, and the detailed synthetic parameters are presented in the Supporting Information. The nanoparticles were isolated by precipitation with methanol. Mixed solvents (THF/methanol) were used to remove the unreacted starting materials, byproducts, and dissociative PS-SH. The resulting precipitate was dried in vacuum to get the final sample.

Characterization. All transmission electron microscopy (TEM) images were recorded using a JEOL JEM-2100 electron microscopy at an accelerating bias voltage of 200 kV. Au NPs was dispersed in THF or toluene. A thick carbon film (20−30 nm) on copper grid was dipped into the solution for a second, dried under atmospheric conditions, and then examined by TEM.

^{1}H SSNMR experiments were performed on a Varian Infinityplus-400 wide-bore (89 mm) NMR spectrometer at a proton frequency of 399.7 MHz. A 2.5 mm T3 double-resonance CPMAS probe was used for ^{1}H SSNMR experiments, and it can provide stable spinning up to 30 kHz within ±2 Hz using a zirconia PENCIL rotor. The magic angle spinning (MAS) frequency used in our experiments was 25 kHz. The ^{1}H chemical shifts were referenced to external TMS. The 90° pulse width was 1.4 μs. Recycle delays between two scans were set to 6 s. The spectra were obtained with 32 scans for each spectrum. The background signal was separately collected under the same condition without sample and then subtracted from the spectra acquired with a sample to obtain all of the spectra used in the subsequent analysis. All of the NMR data were processed with Varian Spinsight software, and all experiments were carried out at room temperature. The temperature controller gas was on during all the experiment to keep the temperature 30 ± 2 °C in the Varian Infinityplus-400 wide-bore (89 mm) NMR spectrometer.

DSC measurements were performed on a Mettler-Toledo DSC1 STARe differential scanning calorimeter with a FRS5 sensor. The samples were heated at a heating rate of 20 °C/min with dry nitrogen as the effluent gas (50 mL/min).

RESULTS AND DISCUSSION

Thiolated polystyrene stabilized gold nanoparticles (PS-S-Au NPs) without surfactant were conveniently prepared by one-phase method, starting from a THF solution of $HAuCl_4{\cdot}3H_2O$ and thiolated polystyrene (PS-SH). By simply changing the synthetic parameters (Table S1, Table S2, and Figure S3), 8 nm, 13 nm PS-S Au NPs (M_n = 2000 g/mol) and 8 nm, 10 nm PS-S Au NPs (M_n = 50 000 g/mol) with high grafting densities of 1.48, 1.25, 0.85, and 1.26 were synthesized (Table S3 and Figure S4). It has been proved that T_g of confined system depended on the different preparation methods. In our research, we chose to use the one-phase method to prepare PS monolayer stabilized Au NPs instead of the two-phase method or ligand exchange reactions, since the latter two kinds of reactions may lead to mixed layers with residual surfactants/short chain thiol at the polymer−Au NPs interface. These residual small molecules may greatly influence the mobility and the glass transition behavior of confined polymers. Morphological characterization by TEM is presented in Supporting Information Figure S3.

A dipolar filter pulse in ^{1}H SSNMR experiments was utilized to study the relative mobility of PS-S- on Au NPs. As shown by a schematic diagram in Figure 1a, the multiple pulse sequence developed by Schmidt-Rohr and co-workers can be used to select the ^{1}H magnetization with weak dipolar−dipolar interaction and suppress the strong ones.[43] With increasing

dx.doi.org/10.1021/ma302643y | Macromolecules 2013, 46, 2292−2297

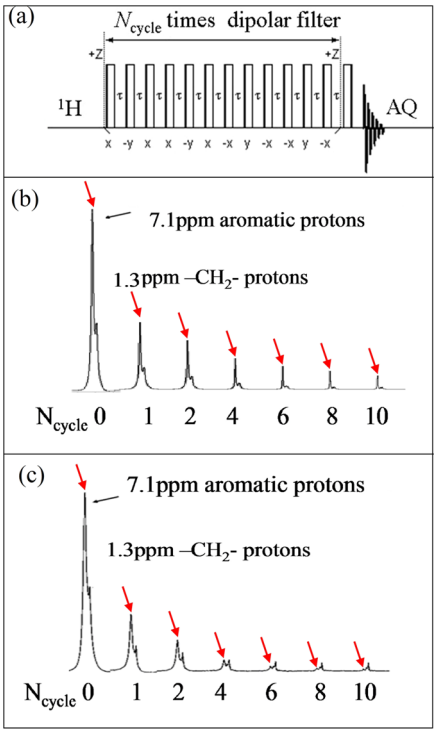

Figure 1. (a) Pulse sequence with a 12-pulse dipolar filter experiment. N_{cycle} indicates the multipulse dipolar filters. Dipolar filtered ^{1}H NMR spectra under 25 kHz MAS for (b) bulk PS-SH and (c) PS-S-Au NPs. M_n = 5300 g/mol.

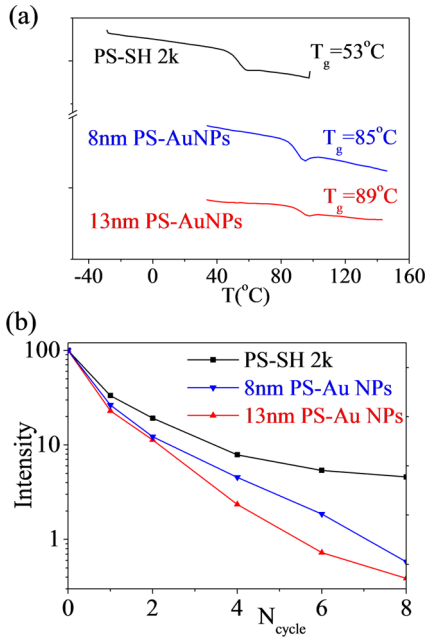

Figure 2. (a) DSC heating curves for bulk PS-SH with M_n = 2000 g/mol and for PS-S- on Au NPs with d = 8 and 13 nm, respectively. T_g is indicated in each curve. (b) Integration NMR signals for aromatic protons versus the N_{cycle} value in dipolar filter ^{1}H NMR experiments for bulk PS-SH and for PS-S-AuNPs with different diameters (M_n = 2000 g/mol).

number of filter cycles (N_{cycle}) more and more signals for rigid components are removed, and the signals for mobile part are selectively observed. Figures 1b and 1c show the dipolar filtered ^{1}HNMR spectra for bulk PS-SH and PS-S-Au NPs (d = 8 nm). Peaks at 7.1 and 1.3 ppm were assigned to the aromatic protons and methylene protons, respectively. As shown in Figures 1b and 1c, NMR signal of aromatic protons for PS-S-Au NPs decayed faster than that for the bulk. For PS-S- (M_n = 5300 g/mol), the mobility of PS-S- on the surface of Au NPs is lower than bulk PS-SH due to the immobilization by the strong interaction between the polymer chains and the surface of Au NPs.

The chain mobility and T_g for bulk PS-SH and PS-S-Au NPs were investigated by NMR dipolar filter experiments and DSC, respectively. In Figure 2a, T_g for bulk PS-SH with M_n = 2000 g/mol and PS-S- on Au NPs with d = 8 nm and d = 13 nm were 53, 85, and 89 °C, respectively. T_g significantly increased up to 36 °C when PS-S- was confined on larger Au NPs. The mobility for PS-SH bulk and those capped on Au NPs were investigated by NMR dipolar filter sequence experiment. The changes in the peak intensities of PS-S- were observed by the dipolar filtered ^{1}H SSNMR experiment, and the data versus N_{cycle} were plotted as shown in Figure 2b. The calculated integral for aromatic proton peaks decayed faster once PS-S- was adsorbed on Au NPs, indicating that the mobility of PS-S- chains was reduced. Moreover, PS-S- adsorbed on larger Au particle (d = 13 nm) showed a larger suppression in NMR peak intensity than that in small particles (d = 8 nm). The same tendency of T_g deviation and that for NMR signal suppression clearly indicate that the surface confinement dominates the glass transition as well as the molecular mobility.

For adsorbed PS-SH with high molecular weight (M_n = 50 000 g/mol), T_g almost remained the same, and no obvious change of chain mobility was observed, as shown in Figure 3. The experimental data by DSC and ^{1}H SSNMR with dipolar filter pulse show little constraints on the adsorbed polymer chains with higher molecular weight.

As indicated in Figures 1−3, ^{1}H SSNMR and DSC studies highlighted several important results: First, compared to bulk PS-SH, the molecular mobility is reduced and T_g increases significantly for PS-S- on Au NPs. Second, the particle size of Au NPs shows important effect on chain mobility and glass transition. PS-S- capped on larger particle seems to be under stronger confinement. Third, the effect of molecular weight of PS-SH has significant influence on the immobilization and glass transition. Fourth, the graft density differs little for different samples, and we demonstrate that confinement effect, which differs for different particle size and molecular weight, is the main reason for the deviation of mobility and T_g. We investigated deviation of T_g for PS-SH with molecular weight ranging from 1000 to 12 000 g/mol on Au NPs (d = 6−8 nm) and plot ΔT_g ($T_g - T_{g,bulk}$) versus molecular weight in Figure 4.

Maccarini and Lennox et al. characterized Au NPs grafted thiol-terminated poly(ethyl oxide) (PEO) in water by means of TEM, thermal analysis, mass density, and small-angle scattering.[52−55] They proposed a core−two shell model for the conformation of PEO. The inner shell was composed almost exclusively of PEO, whereas the outer shell contained polymer and the hydrating water molecules. In this report we investigated molecular mobility and glass transition of PS capped on Au NPs by means of ^{1}H SSNMR and DSC. We found the reduction of mobility and increase in glass transition for short chains of PS-S- on Au NPs, as shown in Figures 1−3. Moreover, the deviations in chain mobility and T_g were found to be molecular weight dependent, as shown in Figure 4. The

dx.doi.org/10.1021/ma302643y | Macromolecules 2013, 46, 2292−2297

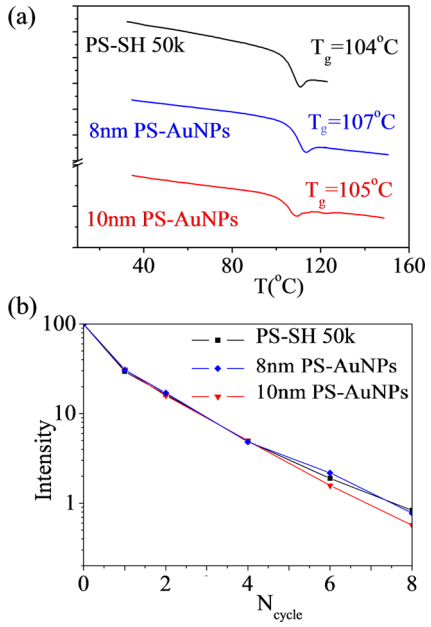

Figure 3. (a) DSC heating curves for bulk PS-SH (M_n = 50 000 g/mol) and the PS-S- capped on Au NPs. (b) Integration of aromatic proton signals versus the N_{cycle} value in dipolar filter ^{1}H SSNMR experiments for bulk PS-SH and PS-S-AuNPs with different diameters (M_n = 50 000 g/mol).

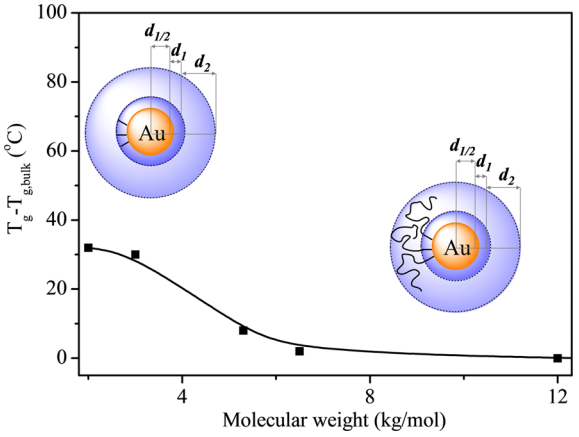

Figure 4. Deviation of T_g for PS-S-Au NPs from their bulk PS-SH. Schematic diagrams of a core−two shell model are inserted in regions of low molecular weight and high molecular weight.

DSC data for polymers grafted on Au NPs can be fitted with the core−two shell model. The inner shell contains about 25 segments of each PS-S- chain nearest to the Au core, which is under strong constraints imposed by confinement. As a result, low molecular weight PS-S- on Au NPs shows a significantly lower mobility and a higher T_g than its bulk polymer. When the high molecular weight of PS-S- were grafted to Au, only a small part of chains are confined in the vicinity of the surface while most chain segments are fitted in the outer shell with less confinement. Thus, the mobility and T_g for high molecular weight PS on Au NPs change little from bulk polymer.

Furthermore, PS-S-Au NPs were incorporated into PS-SH host (1.2 wt %), and T_g for such PNCs was studied. PS-S-Au NPs (10 nm) prepared by the one-phase method readily dispersed in bulk PS-SH by simply codissolution of Au NPs and PS-SH in THF, forming a macroscopically homogeneous red dark-red solution. As is known, observations of significant enhanced thermal or mechanical properties at very low volume fractions of added nanoparticles have motivated an increasing number of investigations.[56] However, further progress is crucially limited by the strong tendency of nanoparticles to aggregate in polymeric matrix.[57,58] Great efforts have been made to achieve high compatibility between the Au NPs and the polymer matrix. Because of the enhancement of stability that long polymer chain offers, coating NPs with polymer layer is a good solution to avoid the strong tendency of NPs to aggregate in polymeric matrix. TEM (Figure 5a) shows that Au

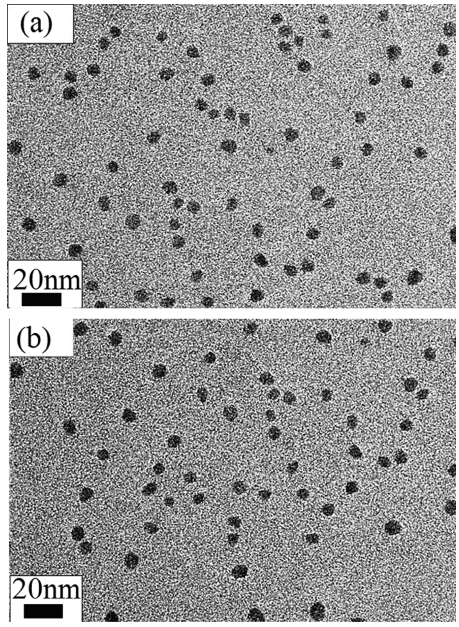

Figure 5. TEM micrographs of (a) composite PS-S-Au NPs (M_n = 12 000 g/mol) in PSH (M_n = 12 000 g/mol). (b) Samples in (a) heated at 160 °C for 4 h.

NPs remain well dispersed in polymer host, without aggregation. The thermal stability of PNCs was tested by heating the composites at 160 °C for 4 h. TEM image Figure 5b indicates that PS-S-Au NPs dispersed into polymer matrix are stable under such thermal conditions, and no aggregation occurs.

To further study the glass transition behavior of PNCs, the DSC thermograms with varied PS-S-Au NPs concentration (wt %) have been examined (shown in Figure 6). For PS-SH (M_n = 2000 g/mol) the presence of less than 1.2% of Au NPs in nanocomposites significantly enhanced the T_g up to 12−17 °C (Figure 6a) while the incorporation of NPs caused no observable change in T_g for PS-SH (M_n = 50 000 g/mol) (Figure 6b). The enhancement of polymer properties by the addition of nanoparticles is a complex function of interfacial interactions, interfacial area, and the distribution of internano-filler distances. Such nanoconfined polymers, conferring significant thermal property improvements, may have more extensive applications than traditional polymer materials.

CONCLUSION

Indeed, despite the effect of nanoscale confinement on T_g has been studied in polymers since 1990s, it is still difficult to find a clear tendency for the glass transition behavior. In most cases, for polymer thin films/polymers confined in nanopores/

dx.doi.org/10.1021/ma302643y | Macromolecules 2013, 46, 2292−2297

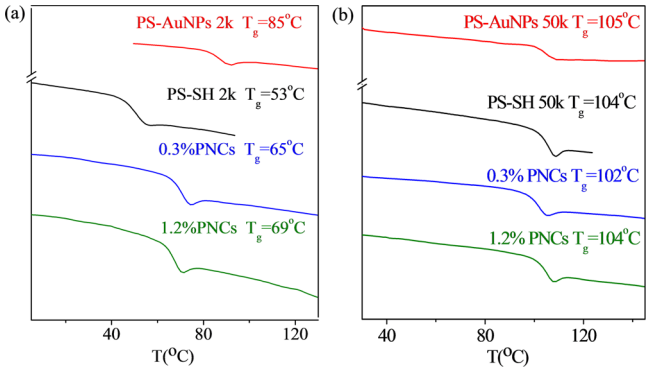

Figure 6. Glass transition temperature measured by DSC for PS-SH host incorporated by PS-S-AuNPs with the same molecular weight. The red and black curves were recorded from neat PS-S-Au NPs and bulk PSSH, respectively. The blue and green lines were recorded from the composites. The concentration of NPs in each PNCs is indicated on each DSC curve.

polymer nanoparticles, confinement usually leads to increased molecular mobility and decreased T_g. Here, a decrease in T_g has not been observed for PS monolayer confined on Au NPs as well as for nanocomposites. In the present work, for the first time we utilized dipolar filter pulse sequence in ^{1}H SSNMR to detect molecular mobility of such nanoconfined polymer systems. The trend of changes in the molecular mobility was consistent with deviation in T_g. Moreover, the size of Au NPs and molecular weight of polymer are two important factors in glass transition for polymer capped nanoparticels as well as for PNCs. This work is essential to better understand the confinement effect, and meanwhile it provides a step toward the ultimate desire to tailor the properties of nanomaterials.

■ ASSOCIATED CONTENT

Ⓢ Supporting Information

Experimental details. This material is available free of charge via the Internet at http://pubs.acs.org.

■ AUTHOR INFORMATION

Corresponding Author

*E-mail xuegi@nju.edu.cn.

Notes

The authors declare no competing financial interest.

■ ACKNOWLEDGMENTS

The author appreciates the financial support of National Basic Research Program of China (973 program, 2012CB821503). This work was also supported by the NSF of China (51133002, 21174062, 21274060).

■ ABBREVIATIONS

PS-SH, thiolated polystyrene; PNCs, polymer nanocomposites; Au NPs, gold nanoparticles; SSNMR, solid-state nuclear magnetic resonance; VFMAS, very fast magic angle spinning; TEM, transmission electron microscopy; DSC, differential scanning calorimetry.

■ REFERENCES

(1) Ellison, C. J.; Torkelson, J. M. *Nat. Mater.* **2003**, *2*, 695−700.
(2) Klein, J.; Kumacheva, E. *Science* **1995**, *269*, 816−819.
(3) Granick, S. *Science* **1991**, *253*, 1374−1379.
(4) Wang, D.; Ishida, H. *C. R. Chim.* **2006**, *9*, 90−98.
(5) Fakhraai, Z.; Forrest, J. A. *Science* **2008**, *319*, 600−604.
(6) Paeng, K.; Swallen, S. F.; Ediger, M. D. *J. Am. Chem. Soc.* **2011**, *133*, 8444−8447.
(7) Lee, H. N.; Paeng, K.; Swallen, S. F.; Ediger, M. D. *J. Chem. Phys.* **2008**, *128*, 10.
(8) Mckenna, G. B. Dynamics of materials at the nanoscale: small molecule liquids and polymer films. In *Polymer Physics: From Suspensions to Nanocomposites and Beyond*; John Wiley & Sons: Hoboken, NJ, 2010; pp 177−209.
(9) Boucher, V. M.; Cangialosi, D.; Alegria, A.; Colmenero, J.; Pastoriza-Santos, I.; Liz-Marzan, L. M. *Soft Matter* **2011**, *7*, 3607−3620.
(10) Stockelhuber, K. W.; Svistkov, A. S.; Pelevin, A. G.; Heinrich, G. *Macromolecules* **2011**, *44*, 4366−4381.
(11) Kim, S.; Torkelson, J. M. *Macromolecules* **2011**, *44*, 4546−4553.
(12) Alcoutlabi, M.; McKenna, G. B. *J. Phys.: Condens. Matter* **2005**, *17*, R461−R524.
(13) Hu, C. W.; Huang, Y. M.; Tsiang, R. C. C. *J. Nanosci. Nanotechnol.* **2009**, *9*, 3084−3091.
(14) Anastasiadis, S. H.; Karatasos, K.; Vlachos, G.; Manias, E.; Giannelis, E. P. *Phys. Rev. Lett.* **2000**, *84*, 915−918.
(15) Kim, T. S.; Dauskardt, R. H. *Nano Lett.* **2010**, *10*, 1955−1959.
(16) Teng, C.; Xue, G. *Acta Polym. Sin.* **2011**, 1001−1006.
(17) Xu, J.; Li, D. W.; Chen, J.; Din, L.; Wang, X. L.; Tao, F. F.; Xue, G. *Macromolecules* **2011**, *44*, 7445−7450.
(18) Eslami, H.; Karimi-Varzaneh, H. A.; Muller-Plathe, F. *Macromolecules* **2011**, *44*, 3117−3128.
(19) Batistakis, C.; Lyulin, A. V.; Michels, M. A. J. *Macromolecules* **2012**, *45*, 7282−7292.
(20) Shin, K.; Obukhov, S.; Chen, J. T.; Huh, J.; Hwang, Y.; Mok, S.; Dobriyal, P.; Thiyagarajan, P.; Russell, T. P. *Nat. Mater.* **2007**, *6*, 961−965.
(21) Katzenstein, J. M.; Janes, D. W.; Hocker, H. E.; Chandler, J. K.; Ellison, C. J. *Macromolecules* **2012**, *45*, 1544−1552.
(22) Rathfon, J. M.; Cohn, R. W.; Crosby, A. J.; Rothstein, J. P.; Tew, G. N. *Macromolecules* **2011**, *44*, 5436−5442.
(23) Eastman, S. A.; Kim, S.; Page, K. A.; Rowe, B. W.; Kong, S. H.; Soles, C. L. *Macromolecules* **2012**, *45*, 7920−7930.
(24) Sun, S. M.; Zhao, L.; Song, Y. H.; Zheng, Q. *Chin. J. Polym. Sci.* **2011**, *29*, 483−489.
(25) Ngai, K. L. *J. Polym. Sci., Part B: Polym. Phys.* **2006**, *44*, 2980−2995.
(26) Forrest, J. A.; Dalnoki-Veress, K. *Adv. Colloid Interface Sci.* **2001**, *94*, 167−196.
(27) Zhang, C.; Guo, Y. L.; Priestley, R. D. *Macromolecules* **2011**, *44*, 4001−4006.
(28) Simon, S. L.; Park, J. Y.; McKenna, G. B. *Eur. Phys. J. E* **2002**, *8*, 209−216.
(29) Rharbi, Y. *Phys. Rev. E* **2008**, *77*, 5.
(30) Robertson, C. G.; Hogan, T. E.; Rackaitis, M.; Puskas, J. E.; Wang, X. *J. Chem. Phys.* **2010**, *132*, 5.
(31) Schonhals, A.; Goering, H.; Schick, C.; Frick, B.; Mayorova, M.; Zorn, R. *Eur. Phys. J.: Spec. Top.* **2007**, *141*, 255−259.
(32) Rittigstein, P.; Priestley, R. D.; Broadbelt, L. J.; Torkelson, J. M. *Nat. Mater.* **2007**, *6*, 278−282.
(33) Elmahdy, M. M.; Chrissopoulou, K.; Afratis, A.; Floudas, G.; Anastasiadis, S. H. *Macromolecules* **2006**, *39*, 5170−5173.
(34) Benkova, Z.; Cifra, P. *Macromolecules* **2012**, *45*, 2597−2608.
(35) Murray, R. W. *Chem. Rev.* **2008**, *108*, 2688−2720.
(36) Daniel, M. C.; Astruc, D. *Chem. Rev.* **2004**, *104*, 293−346.
(37) Hasan, M.; Bethell, D.; Brust, M. *J. Am. Chem. Soc.* **2002**, *124*, 1132−1133.
(38) Badia, A.; Demers, L.; Dickinson, L.; Morin, F. G.; Lennox, R. B.; Reven, L. *J. Am. Chem. Soc.* **1997**, *119*, 11104−11105.
(39) Schmitt, H.; Badia, A.; Dickinson, L.; Reven, L.; Lennox, R. B. *Adv. Mater.* **1998**, *10*, 475−480.
(40) Milette, J.; Cowling, S. J.; Toader, V.; Lavigne, C.; Saez, I. M.; Lennox, R. B.; Goodby, J. W.; Reven, L. *Soft Matter* **2012**, *8*, 173−179.

(41) Rawal, A.; Kong, X. Q.; Meng, Y.; Otaigbe, J. U.; Schmidt-Rohr, K. *Macromolecules* **2011**, *44*, 8100−8105.
(42) Schmidt-Rohr, K.; Spiess, H. W. *Multidimensional Solid-State NMR and Polymers*; Academic Press Inc.: San Diego, 1994.
(43) Egger, N.; Schmidt-Rohr, K.; Blumich, B.; Domke, W. D.; Stapp, B. *J. Appl. Polym. Sci.* **1992**, *44*, 289−295.
(44) Calucci, L.; Forte, C.; Galleschi, L.; Geppi, M.; Ghiringhelli, S. *Int. J. Biol. Macromol.* **2003**, *32*, 179−189.
(45) Sun, P. C.; Dang, Q. Q.; Li, B. H.; Chen, T. H.; Wang, Y. N.; Lin, H.; Jin, Q. H.; Ding, D. T.; Shi, A. C. *Macromolecules* **2005**, *38*, 5654−5667.
(46) Guo, M.; Zachmann, H. G. *Polymer* **1993**, *34*, 2503−2507.
(47) Guo, M. M. *Trends Polym. Sci.* **1996**, *4*, 238−244.
(48) Gu, Q. A.; Wang, X. L.; Sun, P. C.; Zhou, D. S.; Xue, G. *Soft Matter* **2011**, *7*, 691−697.
(49) Wang, X. L.; Gu, Q.; Sun, Q.; Zhou, D. S.; Sun, P. C.; Xue, G. *Macromolecules* **2007**, *40*, 9018−9025.
(50) Vanderhart, D. L.; Manders, W. F.; Stein, R. S.; Herman, W. *Macromolecules* **1987**, *20*, 1724−1726.
(51) Wang, X. L.; Tao, F. F.; Sun, P. C.; Zhou, D. S.; Wang, Z. Q.; Gu, Q.; Hu, J. L.; Xue, G. *Macromolecules* **2007**, *40*, 4736−4739.
(52) Dorris, A.; Rucareanu, S.; Reven, L.; Barrett, C. J.; Lennox, R. B. *Langmuir* **2008**, *24*, 2532−2538.
(53) Oh, H.; Green, P. F. *Nat. Mater.* **2009**, *8*, 139−143.
(54) Corbierre, M. K.; Cameron, N. S.; Sutton, M.; Laaziri, K.; Lennox, R. B. *Langmuir* **2005**, *21*, 6063−6072.
(55) Sih, B. C.; Wolf, M. O. *Chem. Commun.* **2005**, 3375−3384.
(56) Vaia, R. A.; Wagner, H. D. *Mater. Today* **2004**, 32−37.
(57) Fischer, S.; Salcher, A.; Kornowski, A.; Weller, H.; Forster, S. *Angew. Chem., Int. Ed.* **2011**, *50*, 7811−7814.
(58) Corbierre, M. K.; Cameron, N. S.; Sutton, M.; Mochrie, S. G. J.; Lurio, L. B.; Ruhm, A.; Lennox, R. B. *J. Am. Chem. Soc.* **2001**, *123*, 10411−10412.